Aerosol Science and Technology

ISSN: 0278-6826 (Print) 1521-7388 (Online) Journal homepage: http://www.tandfonline.com/loi/uast20

Deposition of Aerosol Particles in Contraction Fittings

Arnold Muyshondt , Andrew R. McFarland & N. K. Anand

To cite this article: Arnold Muyshondt , Andrew R. McFarland & N. K. Anand (1996) Deposition of Aerosol Particles in Contraction Fittings, Aerosol Science and Technology, 24:3, 205-216, DOI: 10.1080/02786829608965364

To link to this article: http://dx.doi.org/10.1080/02786829608965364

Deposition of Aerosol Particles in Contraction Fittings

Arnold Muyshondt, Andrew R. McFarland,† and N. K. Anand*
AEROSOL TECHNOLOGY LABORATORY, DEPARTMENT OF MECHANICAL ENGINEERING,
TEXAS A&M UNIVERSITY, COLLEGE STATION, TX 77843

ABSTRACT. Particle deposition was measured in contraction fittings with half-angles of 12°, 45°, and 90°. It was found that for a given contraction half angle, the losses in a contraction fitting correlate well with the parameter $Stk(1-A_o/A_i)$ where: Stk is a Pich-type Stokes number based on inlet velocity and outlet diameter, A_o is the outlet area, and A_i is the inlet area. A correlation developed from the experimental results allows prediction of the particle losses in contraction fittings as a function of Stokes number, area ratio, and contraction half-angle. Test conditions on which the correlation was based include a range of $0.001 \leq Stk(1-A_o/A_i) \leq 100$. Area ratios A_o/A_i used in the tests were 0.062, 0.215, and 0.571, and the test conditions encompassed Reynolds numbers based on downstream port diameter of 1120 to 58,500. The aerosol particle deposition in the contraction fitting was also modeled numerically and the numerical results show good agreement with the experimental data. Flow turbulence was taken into account in the numerical work using a standard k-e closure model. AEROSOL SCIENCE AND TECHNOLOGY 24:205–216 (1996)

INTRODUCTION

When continuous extractive aerosol sampling from stacks and ducts is used to monitor emissions of particulate matter, aerosol particle losses in transport lines can degrade the quality of results. Currently, the U.S. Environmental Protection Agency (EPA) mandates continuous emissions monitoring (CEM) for those stacks and ducts of the nuclear industry that can potentially emit significant quantities of radionuclides (U.S. EPA 1994a, 1994b). EPA stipulates that sampling methodology shall be performed following the recommendations of ANSI Standard N13.1 (ANSI 1969), which, in turn, requires an evaluation of losses in aerosol transport lines. The U.S. Nuclear Regulatory Commission (NRC) has given approval for its licensees to use DEPOSITION software (Anand et al. 1993) as a means for evaluating line losses (U.S. NRC 1992). Also EPA has recently given the U.S. Department of Energy (DOE) permission to use Alternate Reference Methodology (ARM) at its facilities in lieu of the requirements of ANSI N13.1 (U.S. EPA 1994c). Under the ARM, losses of aerosol particles in the transport lines must be evaluated with the DEPOSITION software. With respect to non-nuclear applications, the U.S. Congress has mandated that EPA setup rules for CEM of incinerators that process over 250 tons/year (U.S. Statutes at Large 1991). If extractive means are used for sampling, it is reasonable to believe that requirements will be imple-

*Current address: Univ. of Arkansas, Fayetville, AR.
†Corresponding author.

Aerosol Science and Technology 24:205–216 (1996)

Published by Elsevier Science Inc.

0278-6826/96/$15.00
SSDI 0278-6826(95)00233-2

Aerosol Science and Technology
24:205–216 April 1996

mented to both minimize and evaluate losses of aerosol particles in transport lines.

A transport system usually consists of a sampling probe, bends (elbows), straight tubes, and in many situations, contraction and expansion fittings. The DEPOSITION code does not currently have the capability of predicting the losses in the latter fittings. Under the present study we have conducted experiments to develop a model for contraction fittings, which will permit modification of DEPOSITION to take into account losses in such fittings.

Aerosol particle deposition in an abrupt contraction has been studied in connection with the human respiratory system (Kim et al. 1984; Itoh et al. 1985) and the modeling of membrane filters and aerosol transport components (Pich 1964; Smutek and Pich 1974; Smith and Phillips 1975; Kanaoka et al. 1979; Ye and Pui 1990; Chen and Pui 1995). Except for the study of Itoh et al., the previous investigations were limited to laminar flow. Also, except for the study of Chen and Pui, all investigations were limited to a 90° half-angle.

In the present research, we conducted a set of experiments over a range of conditions that includes turbulent flow, different angles, and different area ratios, as a means of generating a data base that could be used to develop a correlation for predicting the aerosol particle losses for turbulent flow in contraction fittings with arbitrary half-angles. In addition to the experimental work, the numerical methodology of Gong et al. (1993) was modified to numerically predict the aerosol particle losses in the contraction fittings.

EXPERIMENTAL PROCEDURE

Figure 1 is a schematic of a contraction fitting. In Fig. 1, d_i is the entrance or inlet diameter, d_o is the outlet diameter, and θ is the contraction half-angle. Half-angles of 12°, 45°, and 90° were used to reduce a 27 mm diameter tube to either a 13 mm or a 6.4 mm diameter tube. Fittings with 45° and a 90° half-angle were also used to reduce a 52-mm-diameter tube to a 13-mm diameter.

The apparatus used to test the contraction fittings is shown in Fig. 2. A nearly monodisperse aerosol was generated with a vibrating jet atomizer (Berglund and Liu 1973) from a mixture of oleic acid, alcohol, and sodium fluorescein (analytical tracer). The freshly generated aerosol was passed by a 10-mCi Kr-85 source to neutralize electrical charge. Mean diameter of the aerosol particles was determined by collecting a sample on an oil-phobic glass slide and then measuring the apparent sizes under a microscope. To correct for gravitational flattening, the resulting mean observed diameter was divided by a factor (1.32) developed by Olan-Figueroa et al. (1982) to obtain the actual aerosol particle diameter. The mean aerodynamic diameter, D_a, of the aerosol particles was calculated from

$$\sqrt{\rho_w C_a} D_a = \sqrt{\rho_p C_p} D_p, \tag{1}$$

where C_a is the Cunningham correction based on the aerodynamic diameter, D_p is the actual particle diameter, ρ_p is the particle density (0.933 g/mL for mixture of sodium fluorescein and oleic acid), and C_p is the Cunningham correction factor based on the actual particle diameter. The aero-

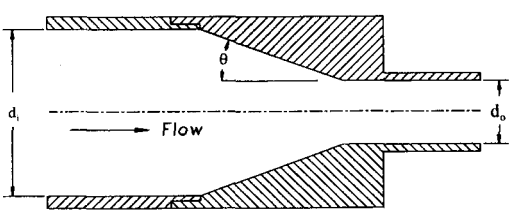

FIGURE 1. Schematic of a contraction fitting.

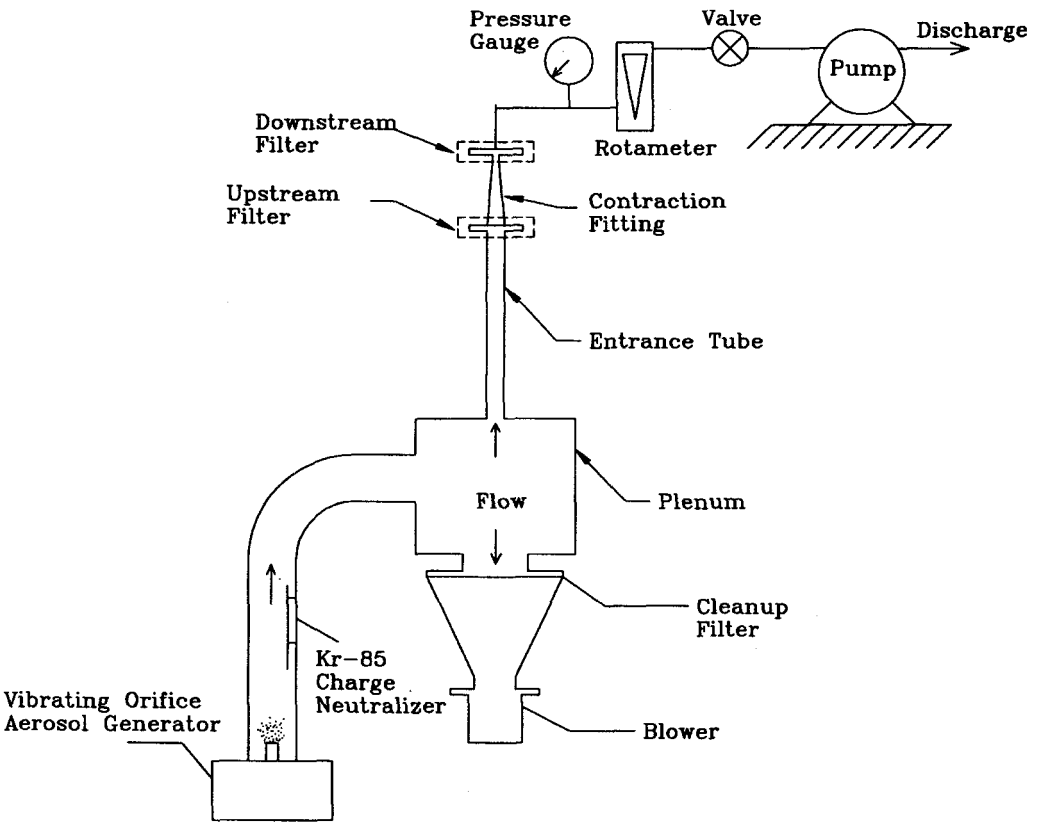

FIGURE 2. Experimental setup for testing contraction fittings. The upstream and downstream filters were alternately inserted into the flow stream during testing.

dynamic particle diameters used in the tests ranged from 5 to 20 μm.

The electrically neutralized aerosol was drawn into a plenum chamber where the flow was split. A portion of the flow was diverted into the vertically-oriented test section while the remaining excess flow was drawn through a cleanup filter and exhausted from the system. To minimize entrance effects, the test flow was drawn into a straight tube that was at least eight diameters in length. A filter sample was first collected at the exit of this section (upstream filter in Fig. 2), then the contraction fitting to be tested was inserted into the flow circuit and a filter sample was collected at its exit plane (downstream filter). This process of collecting filter samples upstream and downstream of the contraction fitting being tested was repeated at least four times for each set of test conditions.

The flow rate was varied in tests of a contraction, and the combination of flow rates and contraction outlet tube sizes gave a range of Reynolds numbers based on the downstream diameter, d_o, of 1,120 to 58,500. Only one data point per area ratio was associated with Reynolds number less than 5,000. To capture the overall effects of the contraction fitting, a two diameter (based on d_e) extension was placed between the fitting and the collection filter.

Aerosol Science and Technology
24:205–216 April 1996

Check tests showed that typically less than 5% of the losses took place in the extension.

Sodium fluorescein was eluted from the sampling filters with a mixture of isopropyl alcohol and water. Three fluorometer readings were taken on aliquots of each filter solution using a Sequoia-Turner Model 450 fluorometer (Sequoia-Turner Corp., Mountain View, CA).

Aerosol penetration through the contraction fitting, P, was calculated from:

$$P = \frac{c_{dn}}{c_{up}} \tag{2}$$

Here c_{dn} is aerosol concentration at the exit plane of the contraction being tested and c_{up} is the aerosol concentration at the exit of the inlet section (no fitting in place). The concentration values were based on fluorometer readings, sampling time, volume of fluid used to elute tracer, and flow rate through the system. The wall losses, Wl, in the contraction fitting were calculated from:

$$Wl = 1 - P. \tag{3}$$

It is the wall loss parameter that will be used as the dependent variable in presenting the results of this study.

NUMERICAL PREDICTIONS

A numerical approach, which includes the effects of turbulence, was used to examine the wall losses in the contraction fitting. The numerical predictions of the particle losses were performed with a model developed by Gong et al. (1993). The assumptions for the analysis are as follows: (1) the concentration of particles in the gas phase is very low; therefore, the particles do not affect the gas flow and particle-particle interactions can be neglected; (2) the mean flow is steady, incompressible, isothermal, and axisymmetric, and (3) the turbulence is isotropic.

The gas flow in a tube with 90°, 45°, and 12° contraction fittings and with area ratios (cross sectional area of the outlet port divided by the cross sectional area of the inlet port) of 0.062, 0.25, and 0.562 were modeled using FIDAP (1993), which is a commercially-available finite element flow solver. An axisymmetric grid with four-node quadrilateral elements was used to generate the geometrical mesh for the solver and a standard κ–ϵ model provided with FIDAP was used to model turbulence. An eight-diameter entrance region was included in the flow domain to match the experimental setup. Computations were made with two different mesh sizes to establish grid independence. Figure 3 shows a sample mesh, velocity vector field, and streamline distribution for a 90° contrac-

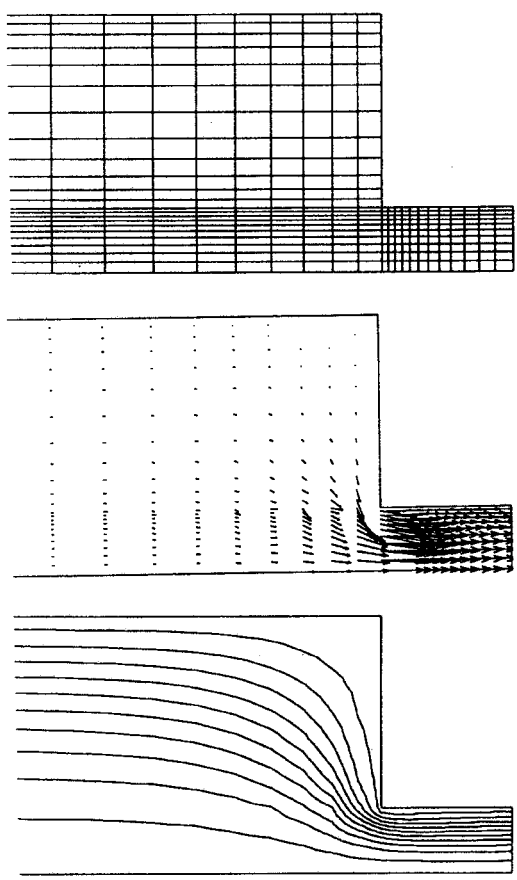

FIGURE 3. Sample computational mesh, velocity vectors, and stream lines for a 90° contraction fitting.

tion fitting. The inlet turbulence intensity was set at 3.5% for the analyses; however, halving or doubling this value did not have a significant influence on the aerosol particle losses in a contraction fitting. The Reynolds number, based on the outlet diameter, for the numerical studies ranged from 15,000 to 113,000.

Lagrangian mechanics were used to compute the particle trajectories. The particle trajectories were predicted by numerically integrating the equations of motion using an explicit numerical scheme. Included in the equations were the effects of drag, particle lift, gravity, and turbulent diffusion. The turbulent diffusion was modeled by assuming the turbulent fluid velocity fluctuations follow a random Gaussian process with a mean of zero and a standard deviation of $(2/3\kappa)^{0.5}$, where κ is the turbulent kinetic energy. The details for the equations of motion and the numerical procedure are given in Gong et al. (1993).

The losses in the contraction fittings were computed by tracking the particle trajectories of two thousand particles. A coefficient of attachment of unity was assumed, i.e., if a particle struck a wall, it adhered to that wall. By counting the number of particles that get deposited on the wall of the contraction fitting, the wall losses, *Wl*, could be evaluated. The number of particles to be tracked was established by successively increasing the number of particles until consecutive results did not vary more than 3%. Similarly, the time step was established by successively decreasing it until there was less than a 3% change between consecutive results.

RESULTS

Pich (1964) showed the deposition of aerosol particles in a 90° contraction can be modeled in terms of a Stokes number based on inlet velocity and outlet diameter, i.e.,

$$Stk = \frac{\rho_p D_p^2 C_p U_i}{9\mu d_o}. \tag{4}$$

Here U_i is the velocity at the inlet of the contraction fitting and μ is the viscosity of air. Ye and Pui (1990) observed that the aerosol particle losses in a 90° contraction were not only a function of the Pich-type Stokes number, *Stk*, but also depended upon the contraction area ratio, A_o/A_i. Ye and Pui also found that the losses in the contraction were independent of the flow Reynolds number. We found that for a constant contraction angle, the wall losses correlated with the parameter $Stk(1 - A_o/A_i)$ rather than the parameter $(Stk/2)^{0.5}/(d_o/d_i)^{0.31}$ suggested by Ye and Pui. The parameter $Stk(1 - A_o/A_i)$ provides plausible asymptotic results—as the area ratio tends to unity (a straight tube) the parameter tends to zero, and as the area ratio tends to zero the parameter approaches the Pich-type Stokes number. It is important to note that the model of Ye and Pui (1990) is limited to laminar flow and is only applicable to 90° contraction half-angles. Also, their model was developed based on numerical studies rather than based upon experimental data as was done in this study.

Plots of the wall losses as a function of $Stk(1 - A_o/A_i)$ for contraction half-angles of 12°, 45°, and 90° are given in Figs. 4–6; respectively. Error bars on the data points represent ± 1 geometric standard deviation about the geometric mean of replicate experiments for a given set of conditions; where the geometric mean, Wl_g, is calculated from

$$\ln Wl_g = \frac{1}{N}\sum_{j=1}^{N} \ln Wl_j. \tag{5}$$

Here N is the number of observations in a data set. The geometric standard deviation, s_g, of a data set is determined from

$$\ln^2 s_g = \frac{1}{N-1}\sum_{j=1}^{N} (\ln Wl_j - \ln Wl_g)^2. \tag{6}$$

The averages of the geometric standard deviations were 1.013, 1.017, and 1.017 for the 12°, 45°, and 90° fittings; respectively.

Aerosol Science and Technology
24:205–216 April 1996

The numerically predicted values of wall losses are included in Figs. 4–6. As may be noted, the numerically predicted wall loss values are in good agreement with the experimental data.

CORRELATION MODEL

The experimentally determined wall loss data in Figs. 4–6 were correlated using an equation of the form

$$Wl = \frac{1}{1 + \left(\frac{X}{ae^{b\theta}}\right)^{c}}, \tag{7}$$

where X is the parameter $Stk(1 - A_o/A_i)$, θ is the contraction half-angle in degrees, and a, b, and c are constants determined by a least-squares procedure. Other equations were evaluated; however, Eq. 7 produced the best fit to the data. The values of the coefficients obtained from the least-squares procedure are

$a = 3.14,$
$b = -0.0185,$
$c = -1.24.$

Equation 7 with these coefficients has a correlation coefficient, r^2, to the experimental data of 0.987. It is noted that as the Stokes number becomes very large, the aerosol particles will travel in a straight line without being influenced by the contraction. For this upper limit, the aerosol particle deposition in contraction fittings will be equal to

$$Wl = \left(1 - \frac{A_o}{A_i}\right). \tag{8}$$

Thus, Equation 7 is only valid up to the limiting value of $Wl = (1 - A_o/A_i)$.

Equation 7 represents a three dimensional surface, which is plotted in Fig. 7 with the experimental data superimposed

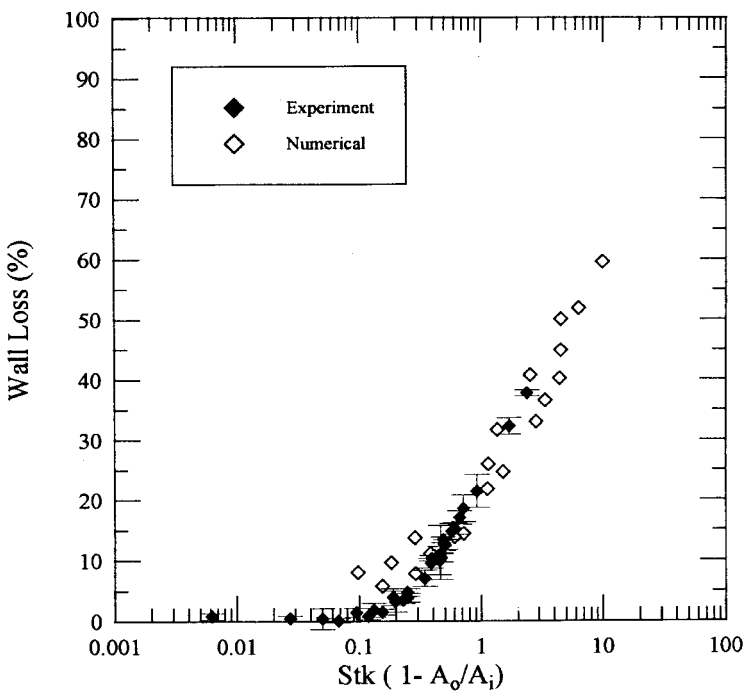

FIGURE 4. Aerosol particle losses for a 12° contraction fitting.

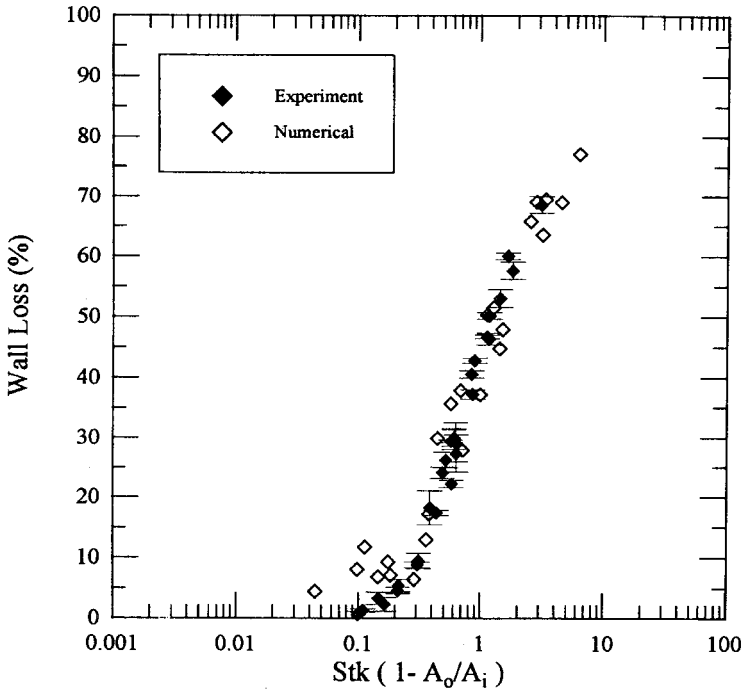

FIGURE 5. Aerosol particle losses for a 45° contraction fitting.

on it. The surface covers the range of independent variables of $0.001 \le Stk(1 - A_o/A_i) \le 100$ and $12° \le \theta \le 90°$.

COMPARISON WITH PREVIOUSLY DEVELOPED MODELS

Given the geometry of the contraction fitting, the flow rate, and the aerodynamic particle diameter, Equation 7 can be used to determine the aerosol particle losses in a contraction fitting. Figures 8–10 show plots of the predicted wall losses for area ratios of 0.0625 and 0.556. Also included in the plots are the losses predicted by the correlations of Pich (1964), Ye and Pui (1990), and Chen and Pui (1995). Although the latter models are based on laminar flow, they were chosen for comparison because, as far as we are aware, there are no general models based on turbulent flow.

The laminar model of Pich for a 90° half angle is of the form

$$Wl = \frac{2Z}{1+G} - \frac{Z^2}{(1+G)^2}, \tag{9}$$

where

$$Z = 2A + 2A^2\left[e^{\left(\frac{-1}{A}\right)} - 1\right], \quad A = Stk\sqrt{G},$$

and $$G = \frac{\sqrt{\frac{A_o}{A_i}}}{1 - \sqrt{\frac{A_o}{A_i}}}.$$

The model was derived by obtaining an approximate analytical solution for laminar flow in the 90° contraction, and then solving the equations of particle motion using the approximate analytical flow solution to obtain the aerosol losses.

Aerosol Science and Technology
24:205–216 April 1996

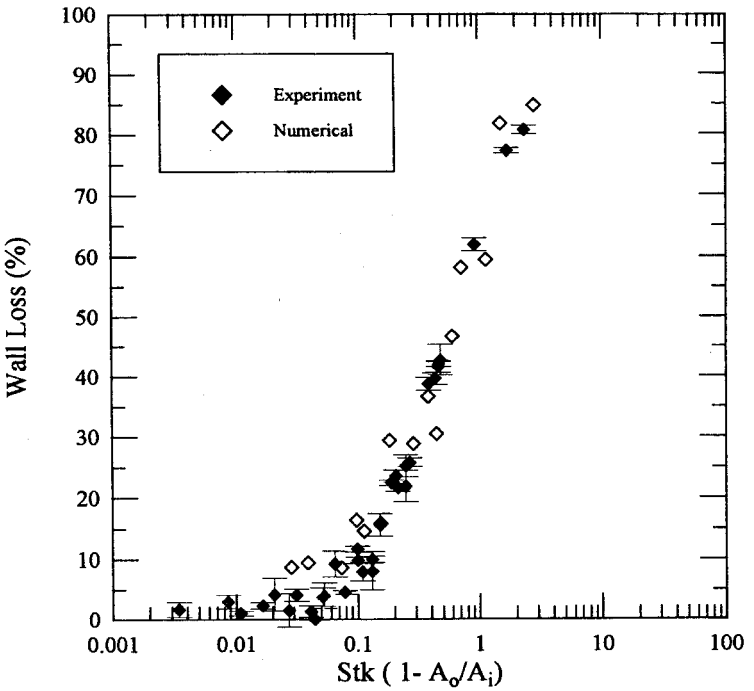

FIGURE 6. Aerosol particle losses for a 90° contraction fitting.

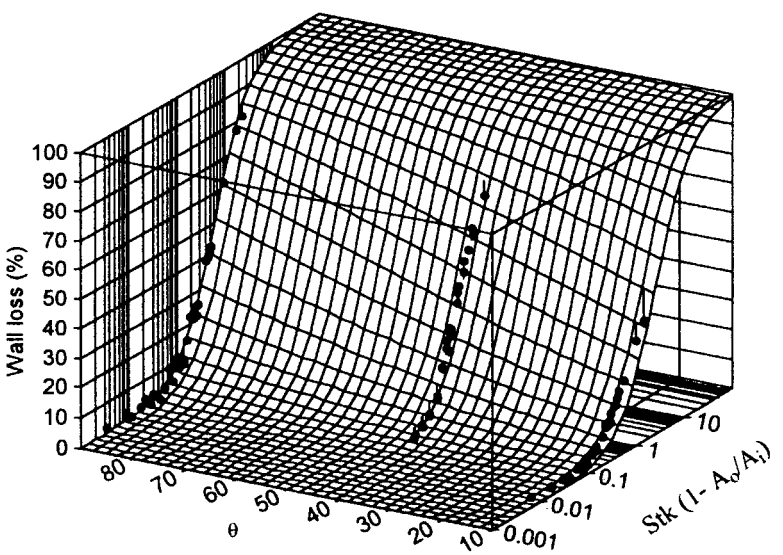

FIGURE 7. Correlation surface for the aerosol particle losses in contraction fittings.

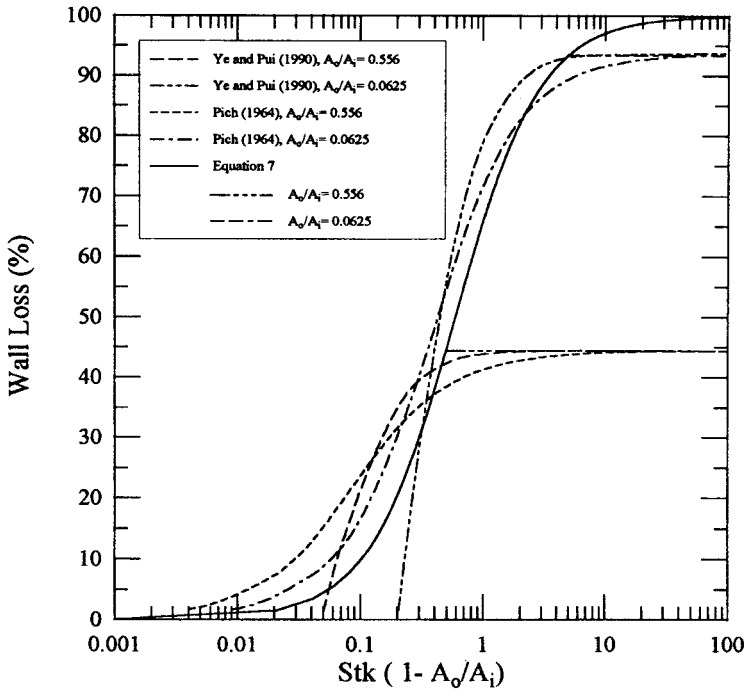

FIGURE 8. Comparison of aerosol particle losses for a 90° contraction fitting predicted by Equation 7 and the models of Pich (1964) and Ye and Pui (1990).

The correlation of Ye and Pui is of the form

$$Wl = \left(1 - \frac{A_o}{A_i}\right)\left[1 - e^{(1.721 - 8.557S + 2.227S^2)}\right], \tag{10}$$

where S is defined as $(Stk/2)^{0.5}/(d_o/d_i)^{0.31}$. Chen and Pui present the following correlation for a contractions with half angles less than 60°:

$$Wl = \left[0.882 + 0.0272y^{0.5} - 8.272y^{0.5}e^{(-3.627y^{0.5})}\right]^2\left[1 - \frac{A_o}{A_i}\right]^2, \tag{11}$$

where

$$y = \frac{Stk\,\sin(\theta)^{1.119}}{0.235\left[\frac{A_i}{A_o}\right]^{0.305}}.$$

With reference to Fig. 8, the 90° half angle models of Pich, and Ye and Pui are compared with the new model for area ratios of 0.0625 and 0.556. As an example, at a value of $Stk(1 - A_o/A_i) = 0.2$, the model of Pich predicts the losses to be 29.7% for an area ratio of 0.062 and 31.5% for an area ratio of 0.56; and, the model of Ye and Pui predicts the losses to be 0% for an area ratio of 0.062 and 35.2% for an area ratio of 0.56. In contrast, the measured losses are approximately 22.6% and our model predicts 20.5% for both area ratios.

Figures 9 and 10 show comparisons of our model to that of Chen and Pui at contraction half-angles of 45° and 12°, respectively. For a 45° half angle and an area ratio of 0.0625 (Fig. 9), the two models produce comparable results except for the asymptotic behavior at larger values of $Stk(1 - A_o/A_i)$. The asymptotes differ because the Chen and Pui model, Eq. 12, has

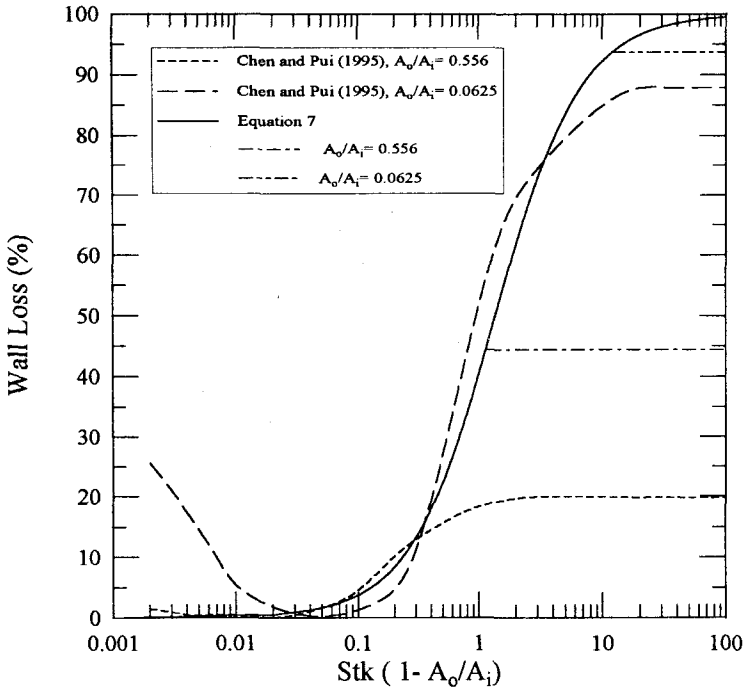

FIGURE 9. Comparison between aerosol particle losses for a 45° contraction fitting predicted by Equation 7 and the model of Chen and Pui (1995).

square terms on the right side, while our limiting value is a first power expression. With reference to Fig. 10, for a 12° half angle and for area ratios of 0.0625 and 0.556, the Chen and Pui model predicts lower values than either our model or data. For example, at value of $Stk(1-A_o/A_i)=1$, and an area ratio of 0.0625, the wall losses predicted by the Chen and Pui model are 8.6%, while those predicted by our model are 24%. The experimentally measured wall losses are 22%. Again, for the half angle of 12°, the asymptotic behavior of the two models is different.

DISCUSSION AND CONCLUSIONS

Aerosol particle losses in contraction fittings were experimentally investigated and a correlation was developed based on the data. For a fixed contraction half-angle, the losses in the contraction fitting correlate well with the parameter $Stk(1-A_o/A_i)$. For values of $Stk(1-A_o/A_i)<0.25$ at $\theta=12°$; $Stk(1-A_o/A_i)<0.15$ at $\theta=45°$; and, $Stk(1-A_o/A_i)<0.05$ at $\theta=90°$ the losses in the contraction fitting are less than 5% and could be considered negligible. However, above these values of $Stk(1-A_o/A_i)$, the losses increase rapidly (up to an asymptotic value of $(1-A_o/A_i)$ and should be taken into account. The aerosol particle losses for a given area ratio, particle size, and flow rate increase with increasing contraction half-angle. Also, in general, the wall losses increase with increasing $Stk(1-A_o/A_i)$, at least up to the limiting value of $1-A_o/A_i$.

The correlation developed from the experimental results was based on 91 tests conducted with three area ratios (0.062, 0.215, and 0.571), a range of particle sizes from 5 to 20 μm aerodynamic diameter, contraction half-angles of 12°, 45°, and 90°, and Reynolds numbers based on outlet diameter of 1120 to 58,500. The correlation,

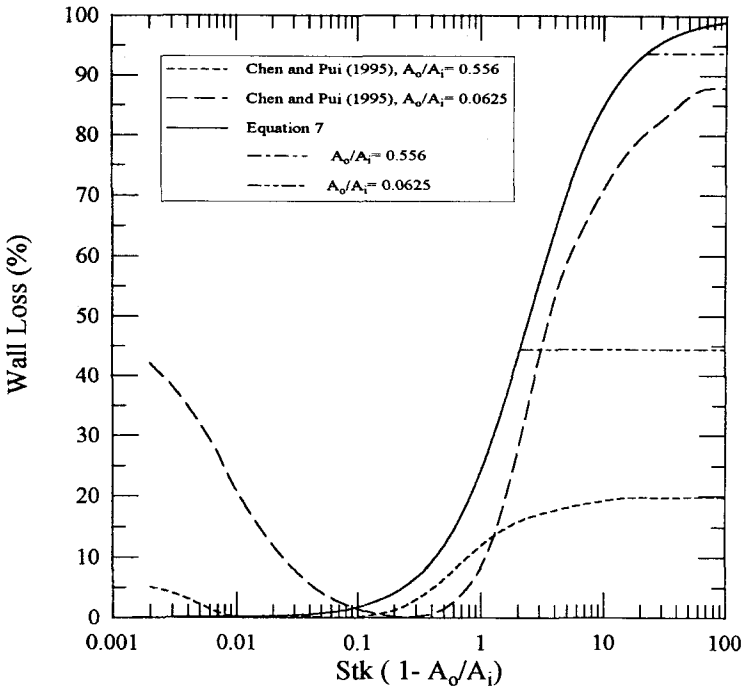

FIGURE 10. Comparison between aerosol particle losses for a 12° contraction fitting predicted by Equation 7 and the model of Chen and Pui (1995).

which covers the range of $0.001 \leq Stk(1 - A_o/A_i) \leq 100$, has a correlation coefficient, r^2, of 0.987. The numerical model used in this study shows good agreement with the experimental results; however, the numerical results show slightly more scatter than the experimental data. This can be partly attributed to the acceptance criterion built into the numerical procedure, whereby a Gaussian random number was used for generating the turbulent fluid velocity fluctuations and we selected a suitable number of particles based on changes in wall losses being less than 3% when the number was increased by a factor of 2. As a consequence, consecutive runs of the numerical procedure for the same contraction geometry, particle size and flow conditions will reflect random variations (on the order of $\pm 2\%$) in the predicted values of wall losses. The numerical predictions show a maximum difference of approximately 11% for all contraction angles when compared to the experimental data. As should be expected for the range of Reynolds numbers for which the tests were conducted, the use of a turbulent flow model improves the prediction accuracy when compared to the laminar models of Pich (1964), Ye and Pui (1990), and Chen and Pui (1995).

The agreement of the experimental and numerical results suggests that losses of aerosol particles in contraction fittings could be determined numerically for conditions that are outside those for which the correlation applies, e.g., a fitting with contoured internal surfaces rather than straight lines. The correlation presented as Eq. 7 should be a useful submodel for predicting the aerosol losses in contraction fittings in a software program such as DEPOSITION.

Funding for this research was provided by the U.S. Nuclear Regulatory Commission (NRC) under Grants NRC-04-92-080 and NRC-04-94-099. Dr. Stephen A.

McGuire is the NRC Project Officer for both grants. The financial and technical support of NRC and Dr. McGuire is gratefully acknowledged.

References

Anand, N. K., McFarland, A. R., Wong, F. S., and Kocmoud, C. J. (1993). *DEPOSITION: Software to Calculate Particle Penetration Through Aerosol Transport Systems*. U.S. Nuclear Regulatory Commission Report NUREG/GR-006. US Government Printing Office, Washington, DC 20402.

American National Standards Institute (1969). *Guide to Sampling Airborne Radioactive Materials in Nuclear Facilities*. ANSI Standard N13.1-1969. New York, American National Standards Institute.

Berglund, R. N., and Liu, B. Y. H. (1973). *Environ. Sci. Technol.* 7:147–153.

Chen, D., and Pui, D. Y. H. (1995). *J. Aerosol Sci.* 26:563–574.

Fluid Dynamics International, Inc. (1993). *FIDAP User's Manual, Revision 7.0*. Evanston, IL.

Gong, H. Anand, N. K., and McFarland, A. R. (1993). *Aerosol Sci. Technol.* 19:294–304.

Itoh, H., Smaldone, G. C., Swift, D. L., and Wagner, H. N. (1985). *J. Aerosol Sci.* 16:167–174.

Kim, C. S., Lewars, G. G., Eldrige, M. A., and Sacker, M. A. (1984). *J. Aerosol Sci.* 15:167–176.

Kanaoka, C., Emi, H., and Aikura, T. (1979). *J. Aerosol Sci.* 10:29–41.

Olan-Figueroa, E., McFarland, A. R., and Ortiz, C. A. (1982). *Am. Ind. Hyg. Assoc.* 43:395–399.

Pich, J. (1964). *Colln. Czech. Chem. Commun.* 29:2223–2227.

Smith, T. N., and Phillips, C. R. (1975). *Environ. Sci. Technol.* 9:564–568.

Smutek, M., and Pich, J. (1974). *Aerosol Sci.* 5:17–24.

U.S. Environmental Protection Agency (1994a). 40 CFR 61 Sub-Part H. National Emissions Standards for Emissions of Radionuclides other than Radon from Department of Energy Facilities. *Code of Federal Regulations*. U.S. Government Printing Office, Washington, DC 20402.

U.S. Environmental Protection Agency (1994b). 40 CFR 61 Sub-Part I. National Emissions Standards for Emissions of Radionuclides from Facilities Licensed by the Nuclear Regulatory Commission and Federal Facilities not Covered by Sub-Part H. *Code of Federal Regulations*. U.S. Government Printing Office, Washington, DC 20402.

U.S. Environmental Protection Agency. (1994c). Letter from Ms. Mary D. Nichols, Assistant Administrator for Air and Radiation, U.S. EPA to Mr. Raymond F. Pelletier, Director, Office of Environmental Guidance, U.S. DOE; dated November 21, 1994.

U.S. Nuclear Regulatory Commission (1992). Air Sampling in the Workplace. Nuclear Regulatory Guide 8.25. U.S. Government Printing Office, Washington, DC 20402.

U.S. Statutes at Large (1991). Public Law 101-549. 104:Part 4. U.S. Government Printing Office, Washington, DC 20402.

Ye, Y., and Pui, D. Y. H. (1990). *J. Aerosol Sci.* 21:29–40.

Received May 24, 1995; revised November 6, 1995